Nuclei Effects on Tip Vortex Cavitation Scaling

S. Gowing, Y. Shen,
Naval Surface Warfare Center Carderock Division, West Bethesda, MD, USA

Abstract
A cavitation susceptibility meter has been used by the US Navy for 16 years to measure the tensile strength of water in the NSWCCD water tunnels, Lake Pend Oreille in Idaho, Exuma Sound in the Bahama Islands, the Pacific Ocean along the US West Coast, and the North Atlantic Ocean. This meter measures the variation of cavitation nuclei with water tension. Using the bubble stability equation, these tensions are related to equivalent size bubbles to produce a spectrum of bubble concentration versus bubble size. This paper compares these nuclei sizes in the lake and ocean waters. Results of bubble dynamics calculations show a relationship for estimating the nuclei effect on scaling that is separate from the viscous effects on the pressure fields. The influence of these nuclei variations on cavitation inception scaling are discussed for a hypothetical propeller tip vortex cavity. The scaling of two model inception conditions are studied for nuclei variations in the model environment as well as variations in the full-scale environment. The sizes of the nuclei in the two environments differ, but the resulting effects on inception are predicted to be minor, and this trend may be globally true for nuclei variations within natural water bodies. The variations illustrated may be minor compared to the nuclei effect for scaling water tunnel model tests to full-scale.

1. Introduction

When a marine propeller operates at high speed, cavitation can occur. Typically the cavitation begins in the vortices that trail off the tips of the blades, then at higher speeds or loadings, the cavitation can occur on the blade surfaces. Because the noise radiated from the cavitation can reveal a ship's position and interfere with the sonar, prediction of the onset speed of tip vortex cavitation is of major interest in naval engineering. The cavitation performance is predicted from model test results that are scaled to full-scale, but this scaling also involves viscous and nuclei effects that are difficult to quantify yet significantly affect the predicted values.

Experimental inception data on tip vortex cavitation show that it is very sensitive to the model size, leading to the prediction of Reynolds number effects [McCormick 1962, Fruman et al 1991, Maines and Arndt 1993]. Because the cavitation process physically requires a weak spot or nucleus for inception, variations of the free-stream nuclei in test facilities also cause variations in model test results even at the same scale [Arndt and Keller 1992, Gowing et al 1995]. Thus nuclei variations can cause model test variations within the same facility, between different model facilities, or between model facilities and the ocean environment. Experiments that try to resolve Reynolds number effects can suffer nuclei effects that make the results difficult to resolve.

2. Previous Efforts for Quantifying Nuclei Effects on Cavitation Scaling

Previous efforts at quantifying the nuclei effect on cavitation have involved measuring the water's cavitation susceptibilty using a Cavitation Susceptibilty Meter (CSM). These devices measure the water's tensile strength with a venturi over a range of cavitation nuclei event rates or concentrations. Operation of the CSM is fairly simple. Water is sucked through a venturi and the flowrate is adjusted with a variable speed pump to vary the venturi throat pressure. When this pressure becomes sufficiently low, bubbles or nuclei in the water cavitate individually and these "events" are detected with an accelerometer or hydrophone. Large bubbles (weak nuclei) cavitate at throat pressures near vapor pressure, and smaller bubbles (strong nuclei) will cavitate in addition to the large ones when the throat pressure decreases further at higher flowrates. By measuring the cavitation event rate over a range of flowrates, the data are converted to a spectrum of cumulative nuclei concentration as a function of tension in the venturi throat. The cumulative nuclei concentration is given by Equation 1, and Equation 2 determines the throat tension.

$$N/v = (N/t)/Q \qquad (1)$$

$$T = P_v - P_t = P_v - (P_0 + Cp_{min}(1/2\rho V_t^2)) \quad (2)$$

in which N/v is the nuclei concentration, N/t is the nuclei event rate, Q is the venturi flowrate, T is the throat tension, P_v is the vapor pressure, P_t is the throat pressure, P_0 is the ambient pressure, Cp_{min} is the pressure coefficient, ρ is the density and V_t is the throat speed.

The venturi's minimum pressure coefficient must be known *apriori* and will vary with throat Reynolds number. This coefficient can be determined by venturi model tests, calculations, or measurements of the cavitation inception point of artificially-injected large bubbles [Chahine and Shen1986, Gindroz et al 1994]. If the cavities in the venturi throat are modeled as bubbles reaching the critical tension determined by the static bubble stability equation, Equation 3, then the specific sizes of the bubbles can be determined. In this equation K is the ratio of specific heats of the bubble gas and s is the interfacial tension of the bubble surface. Assuming that the nuclei in different test facilities or water bodies are primarily bubbles, the CSM will indicate the relative ratios of the ambient bubble sizes in those bodies at similar cavitating conditions. While previous comparisons of bubble-measuring devices have shown that venturi CSMs usually *undercount* bubbles, they still provide information about the relative differences of nuclei between different water sources or changes of water quality within the same source [Gindroz and Briancon-Marjollet 1992].

There are different ways in which the CSM data can then be used to quantify tension or nuclei effects. Gindroz and

$$\frac{1-3K}{3K}\cdot\frac{2s}{R_0}\cdot\left[\frac{3K\left(P_0-P_v\right)}{2s}R_0+3K\right]^{-1/(3K-1)}=T \quad (3)$$

Billet [1994] describe a physically-intuitive approach in which a CSM measures the cumulative nuclei concentrations over a range of tension for a few conditions of water quality, and cavitation inception data for the model are collected at the same time. The water quality conditions can be adjusted by changing the air content or pressure history. Based on the cavitation event rate that defines inception and an estimate of the water flow through the cavitating low-pressure zone, a nuclei concentration is calculated that corresponds to the observed cavity event rate at inception. These events can be visual or acoustic. The tension corresponding to the incipient nuclei concentration is determined from each of the CSM nuclei spectra, and the set of tension values are normalized by the dynamic pressure of the model test. The model's cavitation inception indices are then compared to the normalized tensions to determine the *sensitivity of the model inception to changes in water tension*,(dσ/dT). This value can then be used to correct the model's inception index to conditions of zero tension or any other tension that the full-scale device may encounter. Interestingly, the measured sensitivities of tip vortex inception to tension changes on both a propeller and a foil were close to one in the BEC tunnel at Val-de-Reuil, showing that the two values are closely related [Gowing et al 1995, Gindroz and Billet 1994]. This utilization of CSM data allows nuclei effects to be quantified independent of viscous effects.

3. Calculation of the Bubble Response to Tip Vortex Pressure Fields at Different Scales

An alternative approach to quantifying nuclei effects is direct calculation of the bubble behavior in the pressure field of the model and full-scale tip vortices. Whereas the previous technique assumes the cavitation events to be singular and distinct, acoustic interpretation of inception for large models involves sound pressure level and frequency measurements that are affected by the bubble behavior as well as simple event rates. Shen et al [2001] have derived a scaling formula that separates the viscous and nuclei effects for tip vortex cavitation. The viscous effects determine the scale effect on the pressure field in which the bubbles respond, and the acoustic behavior of different size bubbles are then calculated in both of those pressure fields. The predicted acoustic trends show the onset of a sharp increase in noise with decreasing ambient pressure, and the threshold pressure at which this occurs will define acoustic inception. For similar inception points, the nuclei scaling effect becomes a unique function of the ratio of the bubble sizes involved in the model and full-scale cavities, and the initial size of the cavitating bubbles in the model environment. These bubble calculations are not universal and must be done for the pressure fields based on a specific model-size scale ratio. The results produce a simple factor named 'G' that is similar to the form of scaling law proposed in the 19th ITTC Cavitation Committee Report.

The CSM data give information about the nuclei sizes, hence the CSM results may be used with the 'G' factor calculations to predict the nuclei effect on scaling model propeller cavitation tests for varied nuclei conditions in both the model and full-scale environment. This approach is very different than the previous one for quantifying nuclei effects. For completeness, the approach to the derivation of the 'G' factor is explained briefly.

4. Tip Vortex Cavitation Inception Scaling and the 'G' Factor

Let σ denote the cavitation index based on the vapor pressure of the fluid. The subscript i denotes the index at inception and 'm' and 'f' differentiate the model and full-scale data, respectively. Let C_{pmin} denotes the minimum pressure coefficient in the trailing vortex. In an ideal flow case, cavitation is assumed to occur when the pressure equals the vapor pressure of the fluid, namely $\sigma_i = - C_{pmin}$. However, in a real fluid, cavitation inception is not detected at $-C_{pmin}$ but at a lower pressure or sigma value. This is because a weak spot or nucleus is required to start the cavitation process and these nuclei require their own additional tension to cavitate. This additional tension or decrease in sigma can be written as,

$$\sigma_I = -C_{pmin} - \Delta\sigma \qquad (4)$$

in which $\Delta\sigma$ denotes the tensile strength effect of the bubbles on cavitation inception. Assume that a tip vortex cavitation index σ_{im} is known from a model test. The full-scale tip vortex inception index σ_{if} is to be predicted from a scaling formula, and it is assumed that the full-scale tip vortex is geometrically similar to the model vortex and tested at the same kinematic condition including identical ambient speed. The full-scale cavitation inception index can also occur at a sigma value below $-C_{pmin}$. The ratio of the inception indices then becomes

$$\sigma_{if} / \sigma_{im} = (-C_{pminf} - \Delta\sigma_f)/(-C_{pminm} - \Delta\sigma_m)$$

$$= (-C_{pminf} / -C_{pminm})\, [1+ \Delta\sigma_f / -C_{pminf}]/[1+ \Delta\sigma_m / -C_{pminm}] \qquad (5)$$

Le Rn denotes the Reynolds number. Based on a method of similarity flow solution, Shen et al [2001] shows that

$$-C_{pminf} / -C_{pminm} = (Rn_f / Rn_m)^{0.4} \qquad (6)$$

Because the Rn_f / Rn_m ratio is known, Equation (6) shows that the ratio of pressure distributions between full-scale and model in the trailing vortices due to fluid viscosity and model size effects.

Next, let 'G' represent the scale effect of gas bubbles on cavitation inception between full-scale and model to be

$$G \equiv [1+ \Delta\sigma_f / - C_{pminf}]/[1+ \Delta\sigma_m / - C_{pminm}] \qquad (7)$$

We have

$$\sigma_{if} / \sigma_{im} = G\, (Rn_f / Rn_m)^{0.4} \qquad (8)$$

Equation 8 is a scaling formula to obtain full-scale cavitation inception values from model measurements.

The numerical values of 'G' have been obtained by Shen et al[2001] using the bubble dynamic calculations described before, and their values depend only on the scale factor, the ratio of the bubble sizes and the initial bubble size in the model test.. Let R_{of} and R_{om} denote the initial bubble sizes responsible for cavitation inception in full-scale and model. Figure 1 shows 'G' vs R_{of} / R_{om} at various values of R_{om} for a scale ratio of 4.0. The results show that the nuclei effects will not change the scaling by more than 17% for initial bubble sizes of 0.5μm to 2.5μm and size ratios as much as 3 between the model and full-scale bubbles. Interestingly, if the size ratio is between 1.5 – 1.6, the initial bubble size does not affect the scaling at all for these initial bubble sizes. Generally speaking, the scale effects become more severe for greater size ratios and smaller sizes in the model scale.

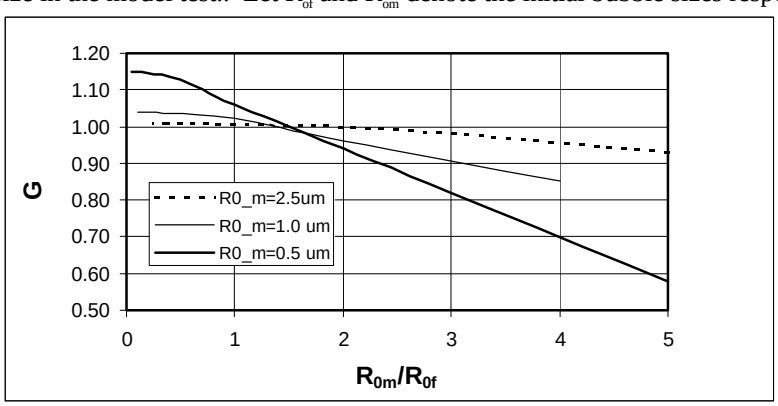

Figure 1. 'G' factor for ¼ scale tip vortices

4. Nuclei Measurements with the CSM

Extensive CSM measurements have been performed using a small venturi at Lake Pend Oreille in Idaho and various parts of the ocean, and a short description of the system is given here. The Lake Pend Oreille, North Atlantic Ocean and Exuma Sound measurements came from a CSM system using a venturi with a throat diameter of 2 mm and a 16:1 area contraction ratio. The overall system was built in two major components. An underwater module housed a variable speed pump, the venturi, and transducers to measure pressure, flowrate and detect cavitation events. A shipboard sub-system controlled the underwater pump and conditioned the signals for recording and display. The two components were connected by an electro-mechanical cable, and a winch lowered the underwater module while the ship was stopped. The Pacific Ocean data were collected from a submarine using the same system except the flow was piped from the outside and the flowrate was adjusted by throttling the sample flow as it passed through the hull into the bilge. More details on this system may be found in Shen et al (1986). Data were collected for a range of cavitation event rates that went from a few to many events per minute. To illustrate, Figure 2 shows data for 6 depths in Lake Pend Oreille. The data were previously used to define a water's susceptibility to cavitation, and the susceptibility was simply the venturi cavitation index at an event rate typical of inception rates (3/min to10/min). Using the 'G' factor to quantify scale effects, however, requires transformation of the CSM data into bubble size data. Figure 3 shows the Pend Oreille CSM data converted to a cumulative bubble spectrum as a function of bubble size using Equations (1 – 3). Most of the bubbles are from 0.5 μm to 2 μm in radius, and their sizes decrease at deeper depths. The North Atlantic Ocean bubbles ranged from 0.1 μm to 1.5μm and the Pacific Ocean bubbles ranged from 0.1 μm to 0.5 μm in radius. Figure 4 shows the locations of the Exuma Sound and North Atlantic Ocean measurements. The Pacific Ocean data were collected off the coast of California.

5. Estimates of Nuclei Scaling Effects from CSM Data

Estimates of the 'G' factor can be made for the scaling of hypothetical model and full-scale cavitation tests in different water bodies using the CSM-derived bubble data. Determination of the bubble sizes and selection of the size relevant to inception followed a sequence of steps. For each CSM data point, the venturi's throat tension was determined and the initial bubble radius R_0 was calculated from the static stability equation. A power law was curve-fit through the resulting spectrum of bubble size versus concentration as shown in Figure 3. The bubble

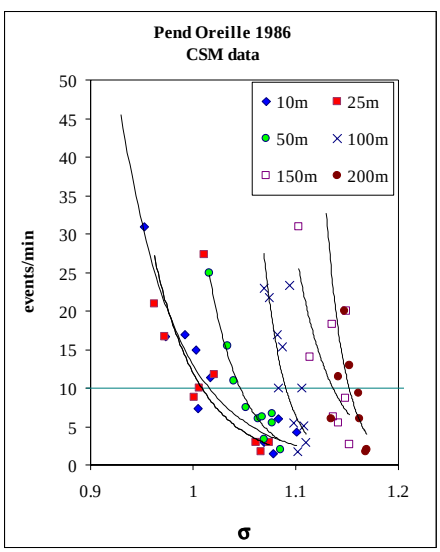

Figure 2. CSM data from Lake Pend Oreille

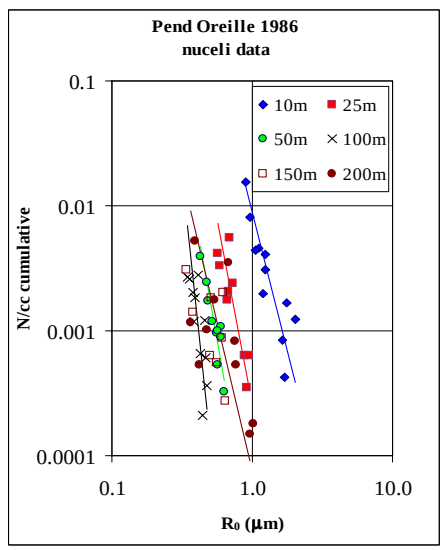

Figure 3. Bubble spectra from CSM data

concentration at the venturi event rate of 10 per minute was determined, and the bubble size corresponding to that concentration was determined from the curve fit. The 10-per-minute rate was chosen as representative of an inception event rate. The ratio of bubble sizes corresponding to this CSM cavitation rate in different water bodies was assumed to be the same as the ratio of bubble sizes in the incipient cavitating tip vortices. The bubble sizes responsible for the model-scale tip vortex inception were assumed to be the same as those for the 10-per-minute inception rate measured in the model water body tests of the CSM. The data for each measurement point (depth, station, year) for all the ocean and lake campaigns were analyzed this way. These data allow the 'G' factor to be estimated.

Not only is the magnitude of the scale effect interesting, but also the variability of this scale effect caused by variability in the nuclei in the same model-test water body at different times, and variability of nuclei from one full-scale water body to another. The magnitude and variability of these effects were calculated for a hypothetical ¼ scale submarine propeller test run in Lake Pend Oreille at different time periods and scaled to different full-scale ocean locations. The 'G' factors are estimated for hypothetical model tests done in each of the 3 years lake data were taken, and the variance of the full-scale predictions are calculated for 5 locations in the North Atlantic Ocean, 4 locations in Exuma Sound and varied locations in the Pacific Ocean. Figures 4a and 4b show the locations of the ocean data. Because no actual model cavitation tests were done during the nuclei measurements, a model cavitation speed of 20 knots was assumed and two inception depths, 10 meters and 25 meters, were chosen. These depths correspond to depths where nuclei data were collected for defining R_{0m}. These conditions also define the model cavitation index. Using the $Re^{0.4}$ scaling and an assumed 'G' factor of 1.0, the full-scale inception index and depth were determined for the same speed. The bubble radius for that depth in the full-scale water body was interpolated from the closest actual data to calculate the R_{0m}/R_{0f} ratio, then the 'G' factor was determined by interpolating in Figure 1 using the R_{0m}/R_{0f} ratio and initial bubble size from the Pend Oreille CSM tests. If the 'G' factor was sufficiently close to 1.0, the actual value was used to calculate the final value of the full-scale inception index and depth. If 'G' was significantly different, then the ratio R_{0m}/R_{0f} was recalculated using the R_{0f} values at the new inception depth and 'G' was again determined. This procedure was iterated until the solutions were similar.

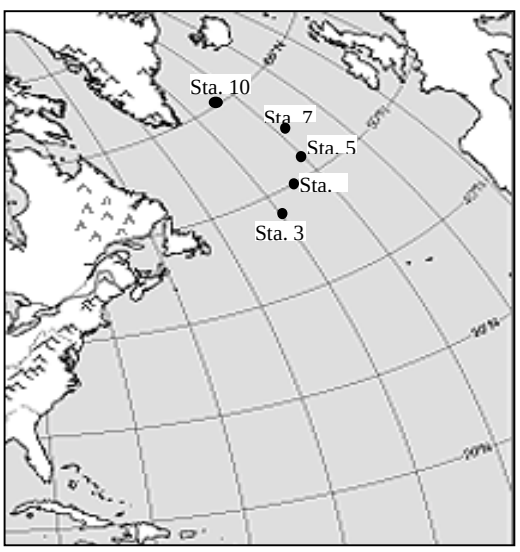

Figure 4a. CSM North Atlantic measurements

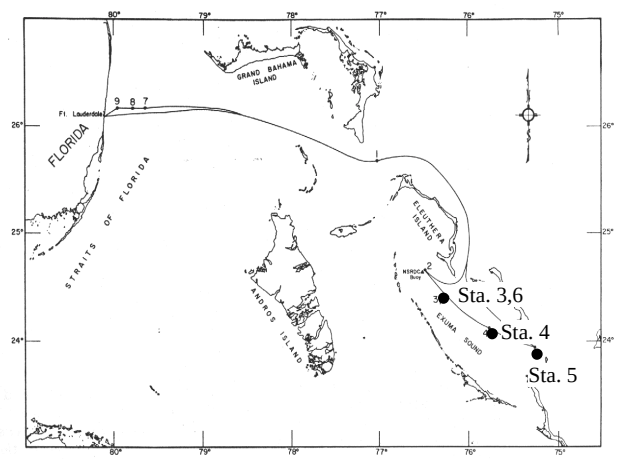

Figure 4b. CSM Exuma Sound measurements

model water tests		full-scale test locations					
Pend Oreille		Exuma Sound 1983					
1985		Depth (m)	Sta. 3	Sta. 4	Sta. 5	Sta. 6	
Depth (m)	R_0 (μm)	25	0.53	0.64	0.94	0.65	
10	1.57	75	0.62	0.57	0.67	1.13	
25	1.21	North Atlantic Ocean 1985					
1986		Depth (m)	Sta. 3	Sta. 4	Sta. 5	Sta. 7	Sta. 10
Depth (m)	R_0 (μm)	25	0.77	1.07	0.49	0.58	0.72
10	1.30	50	0.54	0.46	0.30	0.46	0.40
25	0.70	100	0.30	0.32	0.28	0.25	0.27
1987		Pacific Ocean 1986					
Depth (m)	R_0 (μm)	Depth (m)	Sta. 1		Sta. 2		
10	1.22	62	0.41		0.49		
25	1.23						

Table 1. Bubble sizes R_0 (μm) from CSM

Table 1 shows the bubble size variations at the 10m and 25m model inception depths over the 3 years CSM data were collected in Lake Pend Oreille. The CSM ocean data were collected at depths that did not exactly correspond to the depths predicted for the scaled cavitation, but the data for the closest measured depths are shown. The bubbles in the lake were generally bigger than the ocean bubbles, and the North Atlantic Ocean had the smallest bubbles measured in the three ocean environments. The trend of the lake bubbles being bigger than the ocean ones may correspond to their shallower depth. Overall the dynamic range of the critical nuclei size ratios is small, preventing the 'G' factor from varying greatly from 1.0. The larger bubble sizes typically found in water tunnels would make the dynamic nuclei size range much larger, resulting in larger size ratios. This would cause greater scale effects from the nuclei ('G' much different than 1.0).

	year of model tests in Lake Pend Oreille					
	1985		1986		1987	
model inception depth (m)	10	25	10	25	10	25
Model σ (V=20 kts)	3.62	6.40	3.62	6.40	3.62	6.40
Full-scale σ (V=20 kts)	7.00	12.37	7.00	12.37	7.00	12.37
Full-scale inception depth (m) (assume G=1)	28	57	28	57	28	57
Exuma Sound	**G**					
Sta. 3	0.94	0.97	0.95	1.02	0.96	0.97
Sta. 4	0.96	0.97	0.97	1.03	0.98	0.97
Sta. 5	0.99	0.99	1.00	1.05	1.00	0.99
Sta. 6	0.96	1.00	0.97	1.06	0.98	1.00
North Atlantic	**G**					
Sta. 3	0.98	0.96	0.99	1.01	0.99	0.96
Sta. 4	1.00	0.94	1.00	1.00	1.01	0.94
Sta. 5	0.93	0.86	0.95	0.92	0.95	0.86
Sta. 7	0.95	0.94	0.96	1.00	0.97	0.94
Sta. 10	0.97	0.92	0.98	0.98	0.99	0.92
Pacific	**G**					
Sta. 2	no data	0.95	no data	1.00	no data	0.95
Sta. 1	no data	0.93	no data	0.98	no data	0.92

Table 2. G factors based on bubble sizes

Table 2 shows the resulting 'G' factors predicted for scaling model inception at 10m and 25m for each of the 3 years of lake data to the various full-scale (ocean) locations. Because the ocean data were not collected at the exact depth predicted for full-scale inception, the bubble sizes at the predicted inception depths were interpolated from the data at the closest depths actually measured.

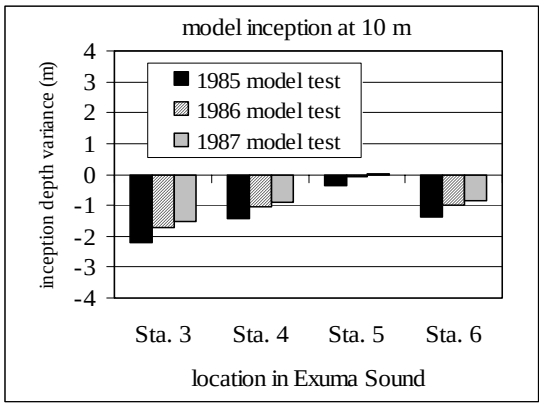

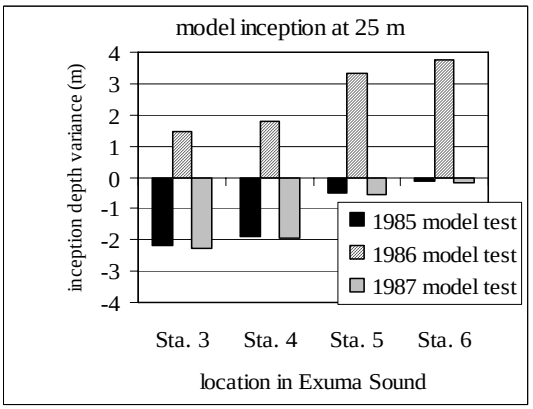

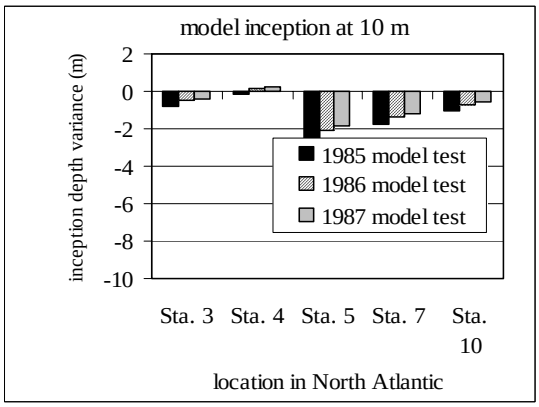

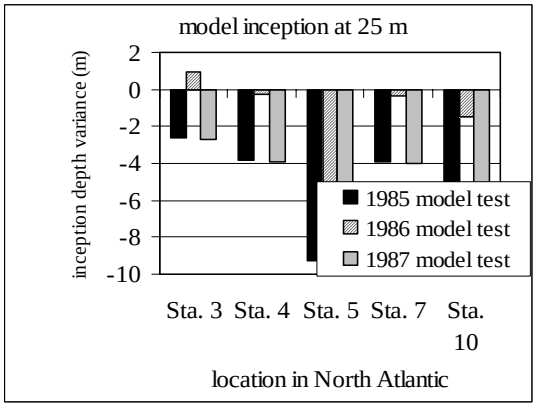

Figure 5. Variations of full-scale inception depth caused by nuclei (variance relative to $Re^{0.4}$ scaling)

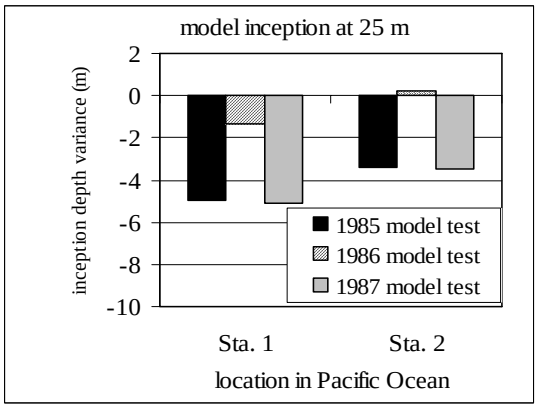

The nuclei effect is typically a variation of 5% or less on the inception index for the measured waters. Most of the R_{0m}/R_{0f} ratios ranged from about 1.3 to 2.5 for the 10 m inception depth case, yielding 'G' factors between 1.0 and 0.90 for R_{0m} = 0.7 μm to 1.6 μm bubbles. For the 25 m depth, the R_{0m}/R_{0f} ratios varied over a greater range from about 0.8 to 3.0, yielding 'G' factors between 1.05 and 0.82. The most extreme size ratios are 0.8 and 4.1, producing 'G' factors of 1.06 to 0.86, respectively. Figure 5 shows the variation in inception depth corresponding to these variations in inception. The depth excursions shown are the differences in depth caused by the nuclei relative to scaling the cavitation purely by the ratio $(Rn_f / Rn_m)^{0.4}$ (G=1.0). Although the variations are not extreme for these

cases, model cavitation inception involving larger bubbles at shallower depths would lead to greater variations than those shown here, or variations in the full-scale water bodies at different times of the year. This exercise simply demonstrates the magnitude of the nuclei scale effect based on these available data.

6. Conclusions

Using bubble dynamic calculations for tip vortices differing by a scale factor, a correction factor has been calculated that predicts the nuclei effect on cavitation inception scaling. The effect depends mostly on the ratio of model and full-scale bubble sizes, as well as the actual size of the model bubbles. Previous data taken with a venturi CSM were analyzed to provide information on the nuclei sizes in a lake and various ocean locations. The nuclei effects on the cavitation scaling of a hypothetical submarine propeller model were estimated for two model cavitation conditions, using model and full-scale nuclei sizes derived from the measured CSM data. The dynamic range of the nuclei size ratios R_{0m}/R_{0f} is small. The change in inception index caused only by nuclei effects is in the order of a few percent, and the most extreme variation is about 18%. These result in variations of up to 10 m in the inception depth. The effect of nuclei variations for the measured data show small variations from one natural water body to another, but these results may be different at shallower or deeper depths or different times of the year. Also, this result may not be true for scaling water tunnel model tests to full-scale environments because the nuclei size ratios may vary much more then the ratios shown here.

Acknowledgements

This work was supported by NAVSEA PMS 450T under the direction of Mr. Larry Becker under the Virginia Class Program.

References

Arndt, R.E.A., Keller, A. 1992 Water Quality Effects on Cavitation Inception in a Trailing Vortex, *J. of Fluids Eng.* **114**.

Chahine, G.L., Shen, Y.T. 1986 Bubble Dynamics and Cavitation Inception in Cavitation Susceptibility Meters, *J. of Fluids Eng.* **108**.

Fruman, D.H., Dugue, C., and Cerruti, P. 1991 Tip Vortex Roll-Up and Cavitation, *ASME Cavitation and Multiphase Flow Forum, FED* **109**.

Gindroz, B., Billard J.Y., Lavigne, S. 1994 Complete Study of a Well-Improved Centerbody Venturi, *2nd International Symposium on Cavitation, Tokyo, Japan.*

Gindroz, B., Briancon-Marjollet, L. 1992 Experimental Comparison between Different Techniques of Cavitation Nuclei Measurement, *Proc. of the 2nd Inter. Symp. on Propellers and Cavitation, Hangzhou, China.*

Gindroz, B., Billet, M.L. 1994 Nuclei and Propellers Cavitation Inception, *Proc. of the ASME FED Symposium on Cavitation, Lake Tahoe, USA*

Gowing, S., Marjollet-Briancon, L., Frechou, D., and Godefroy, V. Dissolved Gas and Nuclei Effects On Tip Vortex Cavitation Inception and Cavitating Core Size, *Int. Symp. on Cavitation CAV '95, Deauville, France.*

Gowing, S., Shen, Y.T. 1987 Cavitation Susceptibilities in Ocean Waters, *David Taylor Naval Ship Research and Development Center Report DTNSRDC-SHD-1241-01*.

McCormick, B.W. 1962 On Cavitation Produced by a Vortex trailing from a Lifting Surface, *J. of Basic Eng*. **84**.

Maines, B.H., and Arndt, R.E.A. 1993 Viscous Effects on Tip Vortex Cavitation, *ASME Symposium on Cavitation Inception, FED* **177**.

Shen, Y.T., Chahine, G., Hsiao, C.T., Jessup, S. 2001 Effects of Model Size and Free-Stream Nuclei on Tip Vortex Cavitation Scaling, *4th Int. Symp. on Cavitation CAV 2001, Pasadena, USA.*

Shen, Y.T., Gowing, S., Eckstein, B. 1986 Cavitation Susceptibility Measurements of Ocean, Lake and Laboratory Waters, *David Taylor Naval Ship Research and Development Center Report DTNSRDC-86/019.*